

Stability of exact solutions of a nonlocal and nonlinear Schrödinger equation with arbitrary nonlinearity

Efstathios G. Charalampidis¹, Fred Cooper^{2,3}, Avinash Khare⁴,
John F. Dawson⁵, Avadh Saxena³

¹Mathematics Department, California Polytechnic State University, San Luis Obispo, CA 93407-0403, United States of America

²The Santa Fe Institute, 1399 Hyde Park Road, Santa Fe, NM 87501, United States of America

³Theoretical Division and Center for Nonlinear Studies, Los Alamos National Laboratory, Los Alamos, NM 87545, United States of America

⁴Physics Department, Savitribai Phule Pune University, Pune 411007, India

⁵Department of Physics, University of New Hampshire, Durham, NH 03824, United States of America

E-mail: echarala@calpoly.edu

E-mail: cooper@santafe.edu

E-mail: avinashkhare45@gmail.com

E-mail: john.dawson@unh.edu

E-mail: avadh@lanl.gov

Abstract. This work focuses on the study of solitary wave solutions to a nonlocal, nonlinear Schrödinger system in 1+1 dimensions with arbitrary nonlinearity parameter κ . Although the system we study here was first reported by Yang (Phys. Rev. E, 98 (2018), 042202) for the fully integrable case $\kappa = 1$, we extend its considerations and offer criteria for soliton stability and instability as a function of κ . In particular, we show that for $\kappa < 2$ the solutions are stable whereas for $\kappa > 2$ they are subject to collapse or blowup. At the critical point of $\kappa = 2$, there is a critical mass necessary for blowup or collapse. Furthermore, we show there is a simple one-component nonlocal Lagrangian governing the dynamics of the system which is amenable to a collective coordinate approximation. To that end, we introduce a trial wave function with two collective coordinates to study the small oscillations around the exact solution. We obtain analytical expressions for the small oscillation frequency for the width parameter in the collective coordinate approximation. We also discuss a four collective coordinate approximation which in turn breaks the symmetry of the exact solution by allowing for translational motion. The ensuing oscillations found in the latter case capture the response of the soliton to a small translation. Finally, our results are compared with numerical simulations of the system.

May 3, 2021 12:46am EST

LA-UR-21-20590

Submitted to: *J. Phys. A: Math. Theor.*

Keywords: Nonlocal nonlinear Schrödinger equation, variational approximation, collective coordinates, dissipation functional, existence and spectral stability analysis.

1. Introduction

The nonlinear Schrödinger equation (NLSE) arises in many areas of physics including Bose-Einstein condensation, plasmas, water waves and nonlinear optics [1], among many others. The possibility of experimentally coupling two-component NLSEs in matrix complex potentials has recently been investigated in nonlinear optics situations in which two wave guides are locally coupled through an antisymmetric medium [2]. In [3, 4], we studied the stability of exact solutions of a single component NLSE in a class of external potentials having supersymmetry (*SUSY*) and parity-time, i.e., \mathcal{PT} symmetry. We then extended our results to two-component NLSEs in \mathcal{PT} -symmetric and supersymmetric external potentials in Refs. [5, 6]. The two-component system we studied in [5] in the absence of the external potential was a particular example of the Manakov system [7] now being studied in the context of nonlocal nonlinear Schrödinger equations (NNLSEs). The NNLSE, its variants and soliton solutions, have been studied in a variety of contexts [8–24].

Here, and upon following Yang’s proposal of imposing the solution constraint $\psi_2(x, t) = \psi_1(-x, t)$, thus rendering the system to become *nonlocal* (see [15]), we generalize these considerations by introducing an arbitrary nonlinearity with exponent denoted as κ hereafter. It should be noted in passing that the resulting system is integrable only for $\kappa = 1$ [15]. In particular, we extend our previous discussion of two coupled NLSEs to the present case in order to compare the nonlocal stability results with those known for the usual one- and two-component *local* NLSEs. A major difference in the solution space is that when we impose the above mentioned constraint, there are no longer moving single soliton solutions; instead they are trapped at the origin. To study the effect of small distortions of the initial solution, we use a variational approximation as well as perform numerical simulations. Small perturbations on an exact solution cause a slight increase in the energy. We find that the domains of stability in terms of the parameter κ are the same as those found for the solitons in the usual Manakov system, where instability occurs for $\kappa > 2$. The collective coordinate (CC) approach gives qualitative agreement for the motion of the perturbed soliton with what is found in numerical simulations of the NNLSE.

The structure of the paper is as follows. In Sec. 2 we present our generalized model and give the exact yet trapped one-soliton solution to the coupled equations. In Sec. 3, we discuss the derivation of the equations of motion from an action principle. The exact solution is given in Sec. 4, and conservation laws resulting from the action are presented in Sec. 5. In Sec. 6 we use both Derrick’s theorem and the Vakhitov-Kolokolov (V-

K) stability criterion to show that for $\kappa > 2$ the solutions are unstable. In Sec. 7 we introduce a 2CC variational approximation and give the equations of motion for these CCs. In Sec. 7.1 we derive the linear response approximation to the CC equations and obtain the small oscillation frequency for the width parameter. The analysis of these equations shows that the soliton is unstable to small oscillations of the width when $\kappa > 2$, a finding that is in full agreement with Derrick's theorem and the V-K criterion. In Sec. 7.2, we give our results for the time evolution in the unstable regime as well as the critical mass when $\kappa = 2$ in the CC approximation. In Sec. 8, we consider a 4CC variational approximation and derive the associated equations of motion. The initial coordinate therein is displaced from the exact solution, and we compare the variational results with numerical simulations of the NNLSE. In Sec. 9 we explain our numerical approach and then compare the numerical results to those of the CC approximation. Finally we state our conclusions in Sec. 10.

2. Yang's version of the nonlocal and nonlinear Schrödinger equation

In [15], special solutions ($\kappa = 1$) of the (generalized) Manakov system:

$$\{i \partial_t + \partial_x^2 + 2g[|\psi_1(x, t)|^2 + |\psi_2(x, t)|^2]^\kappa\} \psi_1(x, t) = 0, \quad (2.1a)$$

$$\{i \partial_t + \partial_x^2 + 2g[|\psi_1(x, t)|^2 + |\psi_2(x, t)|^2]^\kappa\} \psi_2(x, t) = 0 \quad (2.1b)$$

were studied. Upon imposing the solution constraint

$$\psi_2(x, t) = \psi_1(-x, t), \quad (2.2)$$

Eqs. (2.1a)-(2.1b) reduce to the single nonlinear and nonlocal Schrödinger equation (NNLSE) of the form:

$$\{i \partial_t + \partial_x^2 + 2g[|\psi(x, t)|^2 + |\psi(-x, t)|^2]^\kappa\} \psi(x, t) = 0, \quad (2.3)$$

whose Lax pair for $\kappa = 1$ [25] reads

$$\partial_x Y(x, t) = \{-i\zeta J + Q(x, t)\} Y(x, t), \quad (2.4a)$$

$$\partial_t Y(x, t) = \{-2i\zeta^2 J + 2\zeta Q(x, t) + iJ[\partial_x Q(x, t) - Q^2(x, t)]\} Y(x, t) \quad (2.4b)$$

together with

$$J = \begin{pmatrix} 1 & 0 & 0 \\ 0 & 1 & 0 \\ 0 & 0 & -1 \end{pmatrix}, \quad Q(x, t) = \begin{pmatrix} 0 & 0 & \psi_1(x, t) \\ 0 & 0 & \psi_2(x, t) \\ -g\psi_1^*(x, t) & -g\psi_2^*(x, t) & 0 \end{pmatrix}. \quad (2.5)$$

We note in passing that $Y(x, t)$ is the Lax vector in the zero curvature representation and ζ is the spectral function. The Lax pair for Eq. (2.3) is obtained by applying Eq. (2.2) to Eq. (2.5), and its existence renders the system to be integrable for $\kappa = 1$ (even though this is a Hamiltonian system for all κ , it is integrable only for $\kappa = 1$).

Using this method, Yang in [15] found not only one-soliton solutions of the form:

$$\psi(x, t) = \frac{\beta}{\sqrt{2}} \operatorname{sech}(\beta x) e^{i\beta^2 t} \quad (2.6)$$

but also two- and three- soliton solutions of the NNLSE, all for $g = 1$ (the focusing case) and $\kappa = 1$ (integrable case). It should be noted that the constraint given by Eq. (2.2) is different from the one first suggested by Ablowitz and Musslimani in [8, 9]; they considered a different system consisting of two coupled nonlinear Schrödinger equations (NLSEs), namely:

$$\{ i \partial_t + \partial_x^2 + 2g \psi_1(x, t) \psi_2(x, t) \} \psi_1(x, t) = 0, \quad (2.7a)$$

$$\{ -i \partial_t + \partial_x^2 + 2g \psi_2(x, t) \psi_1(x, t) \} \psi_2(x, t) = 0. \quad (2.7b)$$

Imposing the solution constraint: $\psi_2(x, t) = \psi_1^*(-x, t)$, Eqs. (2.7a)-(2.7b) reduce to the single nonlocal and nonlinear equation:

$$\{ i \partial_t + \partial_x^2 + 2g \psi(x, t) \psi^*(-x, t) \} \psi(x, t) = 0. \quad (2.8)$$

The advantage of the system proposed by Yang is that it is accessible in nonlinear optics, and the first three conserved quantities are real by construction. Also the stability of the solutions can be studied using techniques we used to study the usual two-component NLSEs [3].

3. Action principle

The Manakov system of Eq. (2.1a) can be written in vector form as

$$\{ i \partial_t + \partial_x^2 + 2g [\Psi^\dagger(x, t) \Psi(x, t)]^\kappa \} \Psi(x, t) = 0, \quad (3.1)$$

with

$$\Psi(x, t) = \begin{pmatrix} \psi_1(x, t) \\ \psi_2(x, t) \end{pmatrix} \in \mathbb{C}^2. \quad (3.2)$$

It can be shown that Eq. (3.1) can be derived from an action principle. Indeed, let

$$\Gamma[\Psi^\dagger, \Psi] = \int dt L[\Psi^\dagger, \Psi] \quad (3.3)$$

be the action of the system where L stands for its Lagrangian given by

$$L[\Psi^\dagger, \Psi] = T[\Psi^\dagger, \Psi] - H[\Psi^\dagger, \Psi], \quad (3.4)$$

with

$$T[\Psi^\dagger, \Psi] = \int dx \frac{i}{2} \left\{ \Psi^\dagger(x, t) [\partial_t \Psi(x, t)] - [\partial_t \Psi^\dagger(x, t)] \Psi(x, t) \right\}, \quad (3.5a)$$

$$H[\Psi^\dagger, \Psi] = \int dx \left\{ |\partial_x \Psi(x, t)|^2 - \frac{2g}{\kappa + 1} [\Psi^\dagger(x, t) \Psi(x, t)]^{\kappa+1} \right\}. \quad (3.5b)$$

Once we impose the constraint of Yang, then Eq. (2.3) can be obtained from the following nonlocal yet one-component action principle:

$$S[\psi, \psi^*] = \int dt L[\psi, \psi^*], \quad \{ \psi, \psi^* \} \in \mathbb{C}, \quad (3.6)$$

$$L[\psi, \psi^*] = T[\psi, \psi^*] - H[\psi, \psi^*], \quad (3.7)$$

with

$$T[\psi, \psi^*] = \frac{i}{2} \int dx \left\{ \psi^*(x, t) [\partial_t \psi(x, t)] - [\partial_t \psi^*(x, t)] \psi(x, t) \right\}, \quad (3.8a)$$

$$H[\psi, \psi^*] = \int dx \left\{ |\partial_x \psi(x, t)|^2 - \frac{g}{\kappa + 1} [|\psi(x, t)|^2 + |\psi(-x, t)|^2]^{\kappa+1} \right\}. \quad (3.8b)$$

This way, the Lagrange's equation of motion

$$\frac{\delta L[\psi, \psi^*]}{\delta \psi^*(x, t)} - \frac{d}{dt} \left[\frac{L[\psi, \psi^*]}{\delta \dot{\psi}_t^*(x, t)} \right] = 0 \quad (3.9)$$

reproduces Eq. (2.3). Note that in the derivation here we used

$$\frac{\delta \psi(-x, t)}{\delta \psi(x', t')} = \delta(x + x') \delta(t - t'), \quad (3.10)$$

which provides a factor of $2g$ multiplying the nonlocal term. The existence of this action formulation immediately leads to the fact that the Hamiltonian H given by Eq. (3.8b) is conserved.

4. Exact solution

The exact one-soliton solution to Eq. (2.3) is given by

$$\psi(x, t) = A(\beta, \gamma) \operatorname{sech}^\gamma(\beta x) e^{i\omega t}, \quad \gamma = 1/\kappa, \quad (4.1)$$

provided that

$$\omega = (\gamma\beta)^2, \quad 2g [2A^2(\beta, \gamma)]^{1/\gamma} = \beta^2 \gamma(\gamma + 1), \quad (4.2)$$

or, explicitly

$$A(\beta, \gamma) = \frac{1}{\sqrt{2}} \left[\frac{\beta^2 \gamma(\gamma + 1)}{2g} \right]^{\gamma/2}, \quad (4.3)$$

with β being kept arbitrary. Note that Eq. (4.1) agrees with Eq. (2.6) when $g = 1$ and $\gamma = 1$.

5. Conservation laws

It is straightforward to see from Eq. (2.3) that for any initial condition, the mass

$$M = \int dx |\psi(x, t)|^2 \quad (5.1)$$

is conserved. For the exact solution of (4.1), M is explicitly given by

$$M(\beta, \gamma) = \frac{1}{2\beta} \left[\frac{\gamma(\gamma + 1) \beta^2}{2g} \right]^\gamma c_1(\gamma), \quad (5.2)$$

where $c_1(\gamma)$ is given in Eq. (A.1a). In addition, the energy (or the Hamiltonian) given by Eq. (3.8b) is also conserved, and for the solution of Eq. (4.1), $E(\beta, \gamma)$ is given by

$$\begin{aligned} E(\beta, \gamma) &= -M(\beta, \gamma) \beta^2 \frac{\gamma^2(2\gamma - 1)}{2\gamma + 1} \\ &= -\frac{\beta}{2} \frac{\gamma^2(2\gamma - 1)}{2\gamma + 1} \left[\frac{\gamma(\gamma + 1) \beta^2}{2g} \right]^\gamma c_1(\gamma). \end{aligned} \quad (5.3)$$

It can be discerned from Eq. (5.3) that $E(\beta, \gamma) < 0$ for $\gamma > 1/2$ or $\kappa < 2$. Moreover, and for $g = 1$, the critical mass M^* emanating from Eq. (5.2) at $\kappa = 2$ is

$$M^* = \frac{\pi}{4} \sqrt{\frac{3}{2}} = 0.9619123726213981 . \quad (5.4)$$

We note in passing that the parity operator has the effect: $\mathcal{P}\psi(x, t) = \psi(-x, t) = \pm\psi(x, t)$ which is satisfied by the exact solution Eq. (2.8) (enjoying even parity) to Eq. (2.3). Moreover, there are other conservation laws that are directly obtainable from the equations of motion for ψ_1 and ψ_2 . These are the two pseudo-masses

$$\begin{aligned} M_{21} &= \int dx \psi_2^*(x, t) \psi_1(x, t) = \int dx \psi^*(-x, t) \psi(x, t) , \\ M_{12} &= \int dx \psi_1^*(x, t) \psi_2(x, t) = \int dx \psi^*(x, t) \psi(-x, t) . \end{aligned} \quad (5.5)$$

For the exact soliton solution [cf. Eq. (2.8)], these two pseudo-masses are equal and also are to the regular mass. However, once we distort the initial state from the exact solution, these two conserved quantities are complex conjugates of one another.

6. Derrick's theorem

Derrick's theorem [26] states that a solitary wave solution of a Hamiltonian dynamical system is stable, if it is stable to scale transformations of the form: $x \mapsto \alpha x$ ($\alpha > 0$) when we keep the mass of the solitary wave fixed. Let us consider solitary wave functions of the form

$$\psi(x, t) = r(x) e^{-i\omega t} , \quad \text{where} \quad r(-x) = r(x) , \quad (6.1)$$

which scale as

$$\psi(x, t) \mapsto \alpha^{1/2} r(\alpha x) e^{-i\omega t} , \quad (6.2)$$

and preserve M . Moreover, the Hamiltonian H scales as

$$H(\alpha) = H_{\text{kin}}(\alpha) - H_{\text{nl}}(\alpha) , \quad (6.3a)$$

$$H_{\text{kin}}(\alpha) = \int dx |\partial_x \psi(x, t)|^2 = \alpha^2 \int dz |\partial_z r(z)|^2 > 0 , \quad (6.3b)$$

$$\begin{aligned} H_{\text{nl}}(\alpha) &= \frac{g}{\kappa + 1} \int dx [|\psi(x, t)|^2 + |\psi(-x, t)|^2]^{\kappa+1} \\ &= \frac{g 2^{\kappa+1} \alpha^\kappa}{\kappa + 1} \int dz [r^*(z) r(z)]^{\kappa+1} > 0 , \end{aligned} \quad (6.3c)$$

and thus we can write it as

$$H(\alpha) = \alpha^2 h_1 - \alpha^\kappa h_2 , \quad h_1 > 0 , \quad h_2 > 0 . \quad (6.4)$$

It can be shown that the minimum of $H(\alpha)$ is $h_1 = (\kappa/2) h_2$, i.e., upon solving $\left. \frac{\partial H(\alpha)}{\partial \alpha} \right|_{\alpha=1} = 0$. The second derivative of $H(\alpha)$ wrt α and evaluated at $\alpha = 1$ gives the stability requirement in question:

$$\left. \frac{\partial^2 H(\alpha)}{\partial \alpha^2} \right|_{\alpha=1} = 2(2 - \kappa) h_1 \geq 0 . \quad (6.5)$$

This result indicates that solutions are unstable to changes in the width, compatible with the conserved mass, when $\kappa > 2$. The case $\kappa = 2$ is a marginal case where it is known that blowup occurs at a critical mass [27].

The exact solution of Eq. (4.1) has the property that it extremizes the Hamiltonian subject to the constraint of fixed mass. For the exact case, we find

$$H_{\text{kin}} = \frac{\gamma^2}{2\gamma + 1} \frac{\beta}{2} \left[\frac{\gamma(\gamma + 1)\beta^2}{2g} \right]^\gamma c_1(\gamma), \quad (6.6a)$$

$$H_{\text{nl}} = \frac{2\gamma^3}{2\gamma + 1} \frac{\beta}{2} \left[\frac{\gamma(\gamma + 1)\beta^2}{2g} \right]^\gamma c_1(\gamma), \quad (6.6b)$$

so that the exact solution is indeed an extremum of the Hamiltonian wrt scale transformations, with $H_1 = (\kappa/2) H_2$.

6.1. Vakhitov-Kolokolov stability criterion

In the case of the NLSE, one can perform a linear stability analysis of the exact solutions, that is, by letting

$$\psi(x, t) = [\psi_\omega(x) + r(x, t)] e^{-i\omega t}. \quad (6.7)$$

To first order in (the small in amplitude) $r(x, t)$, we arrive at

$$\partial_t r(x, t) = A_\omega r(x, t), \quad (6.8)$$

and this way, one can study the eigenvalues of the differential operator A_ω . If the spectrum of A_ω is imaginary, then the solutions are spectrally stable. Vakhitov and Kolokolov (V-K) showed in [28] that when the spectrum is purely imaginary, then $dM(\omega) / d\omega < 0$ holds. Alongside, they showed that when

$$dM(\omega) / d\omega > 0, \quad (6.9)$$

there is a real positive eigenvalue, thus rendering the solution to be linearly unstable. Assuming that the same argument holds for the NNLSE, we have the following result from the V-K criterion [cf. Eq. (6.9)]: For the solutions of Eq. (4.1) with $\omega = -\gamma^2\beta^2$, we find from (5.2) that

$$M(\omega, \gamma) = \frac{\beta^{2\gamma-1}}{2} \left[\frac{\gamma(\gamma + 1)}{2g} \right]^\gamma c_1(\gamma) = \frac{(-\omega)^{\gamma-1/2} \gamma}{2} \left[\frac{(\gamma + 1)}{2\gamma g} \right]^\gamma c_1(\gamma), \quad (6.10)$$

so that

$$\frac{\partial M(\omega, \gamma)}{\partial \omega} = \frac{1}{2}(1/2 - \gamma) (-\omega)^{\gamma-3/2} \gamma \left[\frac{(\gamma + 1)}{2\gamma g} \right]^\gamma c_1(\gamma), \quad \omega < 0. \quad (6.11)$$

Thus for $\gamma < 1/2$ or $\kappa > 2$ the solitary waves are unstable. This agrees with the result of Derrick's theorem.

7. 2CC variational ansatz

The NNLSE of Eq. (2.3) is invariant under the parity transformation $x \rightarrow -x$, and since the exact solution (4.1) is even under parity, we choose a variational ansatz of the form:

$$\tilde{\psi}[x, Q(t)] = A(t) \operatorname{sech}^\gamma[x/G(t)] \exp[i(-\theta(t) + \Lambda(t)x^2)]. \quad (7.1)$$

We note that Eq. (7.1) is also even under parity, i.e., $\tilde{\psi}[-x, Q(t)] = \tilde{\psi}[x, Q(t)]$. This way, the conserved mass is given by

$$M = \int dx |\tilde{\psi}(x, Q(t))|^2 = G(t) A^2(t) c_1(\gamma), \quad (7.2)$$

where $c_1(\gamma)$ is given in Eq. (A.1a). So $A(t)$ and $G(t)$ are not independent variables, and we can set $A^2(t) = M/[G(t) c_1(\gamma)]$. Since the phase $\theta(t)$ does not enter in the dynamics, it is ignored, thus leaving two independent CCs:

$$Q^\mu(t) = \{ G(t), \Lambda(t) \}. \quad (7.3)$$

We choose initial conditions so as to agree with the exact solution of Eq. (4.1) apart from a small perturbation of $\Lambda(t)$ at $t = 0$:

$$G(0) = G_0, \quad \Lambda(0) = \Lambda_0, \quad A(0) = A_0 = \frac{1}{\sqrt{2}} \left[\frac{\gamma(\gamma+1)}{2gG_0^2} \right]^{\gamma/2}, \quad (7.4)$$

with G_0 being arbitrary and $\Lambda_0 = 0.01$. This way, and as per the above initial conditions for the 2CC ansatz, the mass is the soliton mass given by:

$$M = G_0 A_0^2 c_1(\gamma) = \left[\frac{\gamma(\gamma+1)}{2gG_0^2} \right]^\gamma \frac{G_0 c_1(\gamma)}{2}, \quad (7.5)$$

and thus the value of G_0 fixes the mass. We usually set $G_0 = 1$.

The Lagrangian for the 2CC variational ansatz of Eq. (7.1) is given by

$$L[Q, \dot{Q}] = T[Q, \dot{Q}] - H[Q], \quad (7.6)$$

where

$$T[Q, \dot{Q}] = -MG^2 \dot{\Lambda} \frac{c_2(\gamma)}{c_1(\gamma)}, \quad (7.7)$$

$$H[Q] = M \left\{ 4G^2 \Lambda^2 \frac{c_2(\gamma)}{c_1(\gamma)} + \frac{\gamma^2}{2\gamma+1} \frac{1}{G^2} - \frac{2\gamma^3}{2\gamma+1} \left(\frac{G_0}{G} \right)^{1/\gamma} \frac{1}{G_0^2} \right\}, \quad (7.8)$$

where $c_2(\gamma)$ is given in Eq. (A.1b). This way, the equations of motion for the variational parameters are then given by:

$$\dot{G} = 4G\Lambda, \quad (7.9a)$$

$$\dot{\Lambda} = -4\Lambda^2 + \frac{1}{G^4} \left\{ 1 - \left(\frac{G_0}{G} \right)^{1/\gamma-2} \right\} \frac{\gamma^2}{2\gamma+1} \frac{c_1(\gamma)}{c_2(\gamma)}. \quad (7.9b)$$

In Fig. 1, we present results for the case with $\kappa = 3/2$, $G_0 = 1$, and $\Lambda_0 = 0.01$. In particular, the left and right panels showcase the temporal evolution of $G(t)$ and $\Lambda(t)$, respectively, where the solid blue and red lines correspond to results of the variational approximation and NNLSE with initial conditions of $\psi(x, 0) = \tilde{\psi}(x, 0)$, for comparison.

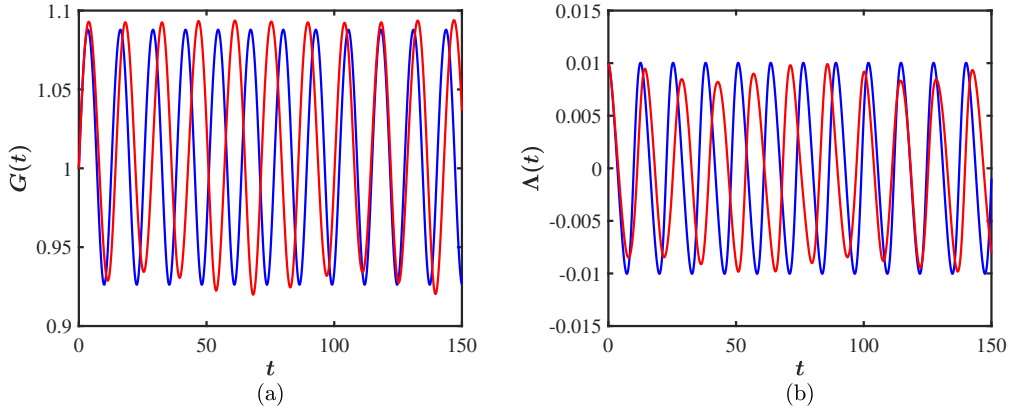


Figure 1. The temporal evolution of $G(t)$ and $\Lambda(t)$ for the 2CC case when $\kappa = 3/2$, with $G_0 = 1$ and $\Lambda_0 = 0.01$. The solid blue and red lines correspond to results obtained from the 2CC approximation [cf. Eqs. (7.9a)] and numerical simulation of the>NNLSE.

The numerical solutions were obtained by using MATLAB's `ODE113` integrator which is a variable-step, variable-order (VSVO) Adams-Bashforth method (see [29], and references therein). We solve the>NNLSE on $x \in [-L, L]$ with $L = 10$ numerically, supplemented by Dirichlet boundary conditions. As per the spatial discretization, we considered a centered yet fourth-order accurate finite difference approximation. We further tested our numerical simulation results by considering other integrators, spatial discretizations, and boundary conditions, such as the `ETDRK4` integrator and Fourier spectral collocation [30], and we obtained essentially similar results. For the 2CC approximation (shown in blue in the figure), $G(t)$ and $\Lambda(t)$ oscillate, indicating stability and agreeing reasonably well with numerical solutions of the>NNLSE (shown in red in the figure).

The conserved energy in the 2CC approximation is expressed as a function of $G(t)$ and $\Lambda(t)$ as follows:

$$E(G, \Lambda, G_0, \gamma) = M(G_0, \gamma) \left\{ 4G^2 \Lambda^2 \frac{c_2(\gamma)}{c_1(\gamma)} + \frac{1}{G^2} \left[1 - 2\gamma \left(\frac{G_0}{G} \right)^{1/\gamma-2} \right] \frac{\gamma^2}{2\gamma+1} \right\}. \quad (7.10)$$

The energy of the perturbed solution is given by its value at $t = 0$

$$E(G_0, \Lambda_0, G_0, \gamma) = M(G_0, \gamma) \left\{ 4G_0^2 \Lambda_0^2 \frac{c_2(\gamma)}{c_1(\gamma)} - \frac{1}{G_0^2} \frac{\gamma^2(2\gamma-1)}{2\gamma+1} \right\}. \quad (7.11)$$

$\Lambda(t)$ oscillates about zero, and when it is at zero, G reaches its maximum value G_m which is determined from its initial energy so that the maximum value that $G(t)$ can have is when $\Lambda(t) = 0$, or when

$$E(G_m, 0, G_0, \gamma) = M(G_0, \gamma) \left\{ \frac{1}{G_m^2} \left[1 - 2\gamma \left(\frac{G_0}{G_m} \right)^{1/\gamma-2} \right] \frac{\gamma^2}{2\gamma+1} \right\}. \quad (7.12)$$

The maximum value of G for $\kappa = 3/2$ when we choose $\Lambda_0 = 0.01$, $G_0 = 1$ is given by $G_m = 1.087874$. This value of G_m is seen in both the 2CC approximation and in the numerical simulations as seen in Fig. 1.

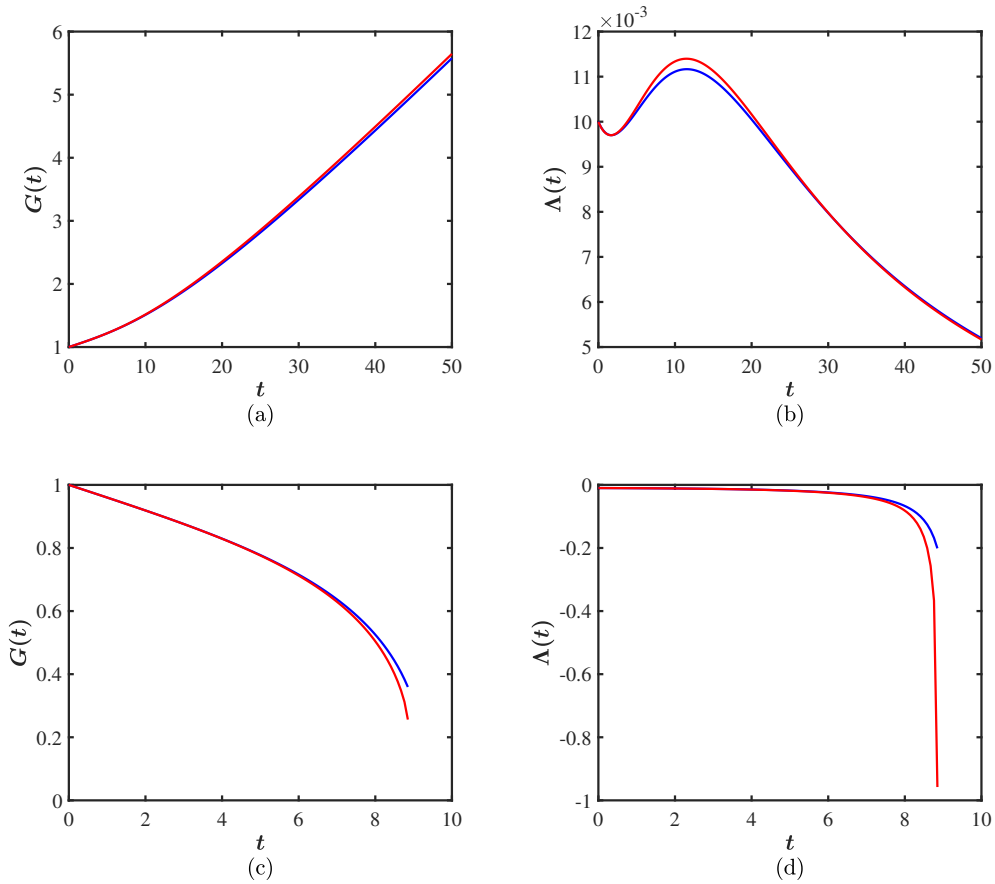


Figure 2. Same as Fig. 1 but with $\kappa = 2.2$ (top panels) and $\kappa = 2.1$ (bottom panels), respectively ($G_0 = 1$ in both cases). In particular, the temporal evolution of $G(t)$ and $\Lambda(t)$ for the 2CC and NNLSE is presented for $\Lambda_0 = 0.01$ (blowup) and $\Lambda_0 = -0.01$ (collapse) in the top and bottom panels, respectively. Similarly, the blue solid line corresponds to the solution of the 2CC approximation [cf. Eqs. (7.9a)] whereas the solid red line to the numerical solution of the NNLSE.

The cases when $\kappa = 2.2$ and $\kappa = 2.1$ are shown in the top and bottom panels of Fig. 2. Specifically, the onset of collapse is presented in the top panels in the figure whereas a case corresponding to blowup is shown at the bottom panels therein. We should note that the numerical solutions agree quite well with the 2CC simulations (shown in red and blue, respectively).

7.1. Linear response

We now discuss the first-order linear response to Eq. (7.9a). To that end, we first set

$$G(t) = G_0 + \Delta G, \quad \Lambda(t) = \Delta \Lambda(t), \quad (7.13)$$

and substitute them into Eq. (7.9a) subsequently. Upon keeping only first-order terms, we arrive at

$$\Delta \dot{G} = 4 G_0 \Delta \Lambda, \quad (7.14a)$$

$$\Delta\dot{\Lambda} = -\frac{\gamma(2\gamma-1)}{2\gamma+1} \frac{c_1(\gamma)}{c_2(\gamma)} \frac{\Delta G}{G_0^5}. \quad (7.14b)$$

Differentiating Eq. (7.14a) wrt t , and replacing $\Delta\dot{\Lambda}$ therein with Eq. (7.14b), we find

$$\Delta\ddot{G} + \omega_G^2 \Delta G = 0, \quad (7.15)$$

where

$$\omega_G^2 = \frac{4\gamma(2\gamma-1)}{2\gamma+1} \frac{c_1(\gamma)}{c_2(\gamma)} \frac{1}{G_0^4}. \quad (7.16)$$

Based on the above, the system is unstable wrt width $G(t)$ if $\gamma < 1/2$ or $\kappa > 2$, a finding that is independent of the value of G_0 and in agreement with Derrick's theorem. For $G_0 = 1$ and $\kappa = 3/2$, the oscillation period $T_G = 2\pi/\omega_G = 12.6$ is in agreement with the stable $G(t)$ oscillations shown in Fig. 1. As per the unstable case with $\kappa = 2.1$, the lifetime $\tau_G = 1/|\omega_G| = 7.6$ is in reasonable agreement with the lifetime shown in Fig. 2.

7.2. Blowup for $\kappa \geq 2$

Within the 2CC approach, we can look at the equation of motion for the width parameter $G(t)$ in order to see if it goes to zero (blowup) or infinity (collapse). It is easiest to look at the energy conservation equation to study these phenomena. If we fix $G_0 = 1$, then from energy conservation and the equation of motion for $G(t)$, the scaled energy of Eq. (3.4) can be rewritten as:

$$\frac{E}{M} = \frac{\dot{G}^2 c_2(\gamma)}{4 c_1(\gamma)} + \frac{1}{G^2} \frac{\gamma^2}{2\gamma+1} - \frac{2\gamma^3}{G^{1/\gamma}(2\gamma+1)}. \quad (7.17)$$

We immediately notice that when $\kappa = 2$, the last two terms cancel so that for the exact solution $\dot{G}(t)$ is constant. To determine a critical mass, one needs to allow for initial conditions with mass greater than the exact solution, and assume a self-similar shape. To this end, we proceed as follows. Let us look first at the case with $\kappa > 2$ where it is possible to have the width parameter $G(t) \rightarrow 0$. Upon rewriting the energy equation as

$$\dot{G}^2 = 4 \frac{c_1(\gamma)}{c_2(\gamma)} \left(\frac{E}{M} + \frac{2\gamma^3}{G^{1/\gamma}(2\gamma+1)} - \frac{1}{G^2} \frac{\gamma^2}{2\gamma+1} \right), \quad (7.18)$$

and considering $G \rightarrow 0$, we can ignore the first and last terms, thus obtaining

$$\dot{G} = -\sqrt{\frac{c_1(\gamma)}{c_2(\gamma)} \frac{2\gamma^3}{G^{1/\gamma}(2\gamma+1)}} \quad (7.19)$$

for blowup. In other words, when we get near the critical time t^* , we have

$$G(t) \propto (t - t^*)^{2/(\kappa+2)}. \quad (7.20)$$

To explore the critical mass, we do not use the exact solution as our starting point. Instead, we rewrite the nonlinear term in terms of the mass M of the solitary wave via

$$A^2(t) \rightarrow M\beta(t)/c_1(\gamma). \quad (7.21)$$

This way, when $q(t) = 0$, we have that

$$\begin{aligned} \tilde{H}_{\text{nl}} &= \frac{g}{\kappa + 1} \int dx [|\tilde{\psi}(x, t)|^2 + |\tilde{\psi}(-x, t)|^2]^{\kappa+1} \\ &= \frac{g \gamma}{\gamma + 1} A^{2/\gamma+2} G \int dy [2 \operatorname{sech}^{2\gamma}(y)]^{1/\gamma+1} = M \frac{2\gamma^2}{2\gamma + 1} \frac{2g}{\gamma + 1} \left(\frac{2M}{G c_1(\gamma)} \right)^{1/\gamma}. \end{aligned} \quad (7.22)$$

For blowup to set in when $\gamma = 1/2$, this term must be bigger than the negative $1/G^2$ term in the energy, so for $g = 1$, one gets the condition:

$$M \geq M^* = \frac{\pi}{4} \sqrt{\frac{3}{2}} = 0.9619123726213981, \quad (7.23)$$

which in turn is in agreement with Eq. (5.4).

8. 4CC variational ansatz

When we displace the position, we destroy the exact parity symmetry of the solutions of the NNLSE. In this section, we study this by choosing a parity-breaking, four collective coordinate (4CC) ansatz for our variational wave function of the form:

$$\tilde{\psi}(x, Q(t)) = A(t) \operatorname{sech}^\gamma[(x - q(t))/G(t)] e^{i\phi(x)}, \quad (8.1a)$$

$$\phi(x, Q(t)) = -\theta(t) + p(t)(x - q(t)) + \Lambda(t)(x - q(t))^2. \quad (8.1b)$$

The mass is again given by $M = G(t) A^2(t) c_1(\gamma)$, so that $A(t)$ can be eliminated in favor of $G(t)$ as an independent variable. Similar to the 2CC case, the phase $\theta(t)$ in the 4CC case does not enter in the dynamics so it can be ignored. Thus, we are left with four variational parameters:

$$Q(t) = \{ q(t), p(t), G(t), \Lambda(t) \}. \quad (8.2)$$

The Lagrangian in this case is given by

$$L[Q, \dot{Q}] = T[Q, \dot{Q}] - H[Q], \quad (8.3)$$

where

$$T[Q, \dot{Q}] = M \left\{ p \dot{q} - G^2 \dot{\Lambda} \frac{c_2(\gamma)}{c_1(\gamma)} \right\}, \quad (8.4a)$$

$$H[Q] = M \left\{ p^2 + 4 G^2 \Lambda^2 \frac{c_2(\gamma)}{c_1(\gamma)} + \frac{1}{G^2} \left[1 - 2\gamma \left(\frac{G_0}{G} \right)^{1/\gamma-2} f(q/G, \gamma) \right] \frac{\gamma^2}{2\gamma + 1} \right\}, \quad (8.4b)$$

together with

$$f(z, \gamma) = \frac{2\gamma + 1}{2^{1/\gamma+2} \gamma c_1(\gamma)} \int dy [\operatorname{sech}^{2\gamma}(y - z) + \operatorname{sech}^{2\gamma}(y + z)]^{1/\gamma+1}. \quad (8.5)$$

Thus, the equations of motion are given by:

$$\dot{q} = 2p, \quad (8.6a)$$

$$\dot{p} = \frac{2\gamma^3}{2\gamma + 1} \frac{1}{G^3} \left(\frac{G_0}{G} \right)^{1/\gamma-2} f'(q/G, \gamma), \quad (8.6b)$$

$$\dot{G} = 4G\Lambda, \quad (8.6c)$$

$$\dot{\Lambda} = -4\Lambda^2 + \left\{ \frac{1}{G^4} \left[1 - \left(\frac{G_0}{G} \right)^{1/\gamma-2} f(q/G, \gamma) \right] - \frac{\gamma q}{G^5} \left(\frac{G_0}{G} \right)^{1/\gamma-2} f'(q/G, \gamma) \right\} \frac{\gamma^2}{2\gamma+1} \frac{c_1(\gamma)}{c_2(\gamma)}. \quad (8.6d)$$

It should be noted in passing that Eqs. (8.6a) agree with the 2CC equations discussed in the previous section when $q = p = 0$.

For the discussion that follows next on the 4CC case, we consider initial conditions of the form of:

$$q_0 = 0.1, \quad p_0 = 0, \quad G_0 = 1, \quad \Lambda_0 = 0. \quad (8.7)$$

Typical results for values of $q(t)$, $p(t)$, $G(t)$, and $\Lambda(t)$ are shown in Fig. 3 for the 4CC ansatz along with the numerical findings of Eq. (2.3) using the same numerical methods as previously. We note that the 4CC ansatz does not preserve parity conservation, and also does not preserve the conservation of the pseudo-masses M_{12} and M_{21} defined in Eq. (5.5). For the shifted solution these pseudo-masses are complex. Although they are conserved for the exact NNLSE, they are not for the 4CC ansatz. Because of this shortcoming, we only present one such result, namely for $\kappa = 1.5$ and $q_0 = 0.1$. Both the 4CC results shown in blue and the numerical solution of the NNLSE shown in red are in substantial agreement. Both oscillate about equilibrium values and indicate stability of the soliton.

9. Numerical simulations of the NNLSE

In this Section, we investigate the stability and spatio-temporal evolution of the exact solution (4.1) to the NNLSE (2.3). To do so, we employ the separation of variables ansatz $\psi(x, t) = \psi^{(0)}(x)e^{i\omega t}$, which is inserted into Eq. (2.3), thus obtaining:

$$\frac{d^2\psi^{(0)}(x)}{dx^2} + 2g \left[|\psi^{(0)}(x)|^2 + |\psi^{(0)}(-x)|^2 \right]^\kappa \psi^{(0)}(x) - \omega\psi^{(0)}(x) = 0. \quad (9.1)$$

Then, Eq. (9.1) is solved by means of a Newton-Krylov method [31] with Eq. (4.1) as an initial guess. Having identified a stationary solution $\psi^{(0)}(x)$ (upon convergence of the Newton-Krylov solver), we perform a spectral stability analysis around it using the ansatz:

$$\tilde{\psi}(x, t) = e^{i\omega t} \left[\psi^{(0)}(x) + \varepsilon \left(a(x)e^{\lambda t} + b^*(x)e^{\lambda^* t} \right) \right], \quad \varepsilon \ll 1. \quad (9.2)$$

Upon inserting Eq. (9.2) into Eq. (2.3) we arrive (at order $\mathcal{O}(\varepsilon)$) at the eigenvalue problem of the form of

$$\begin{pmatrix} A_{11} & A_{12} \\ -A_{12}^* & -A_{11}^* \end{pmatrix} \begin{pmatrix} a \\ b \end{pmatrix} = \tilde{\lambda} \begin{pmatrix} a \\ b \end{pmatrix}, \quad \tilde{\lambda} = -i\lambda, \quad (9.3)$$

with matrix elements given by

$$A_{11} = \frac{d^2}{dx^2} + 2g \left\{ \kappa \left[|\psi^{(0)}(x)|^2 + |\psi^{(0)}(-x)|^2 \right]^{\kappa-1} \left[|\psi^{(0)}(x)|^2 + \psi_0(x)\psi_0^*(-x)\mathcal{P} \right] + \left[|\psi^{(0)}(x)|^2 + |\psi^{(0)}(-x)|^2 \right]^\kappa \right\} - \omega,$$

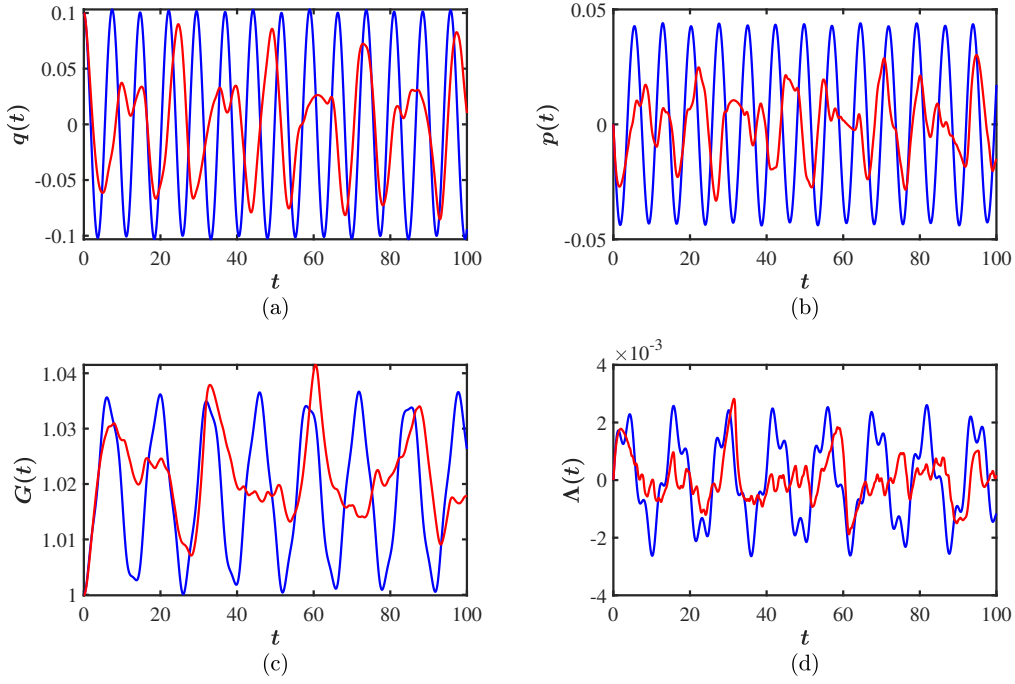


Figure 3. Same as Fig. 1 but for the 4CC case with $\kappa = 3/2$ and $G_0 = 1$. In particular, the temporal evolution of $q(t)$, $p(t)$, $G(t)$, and $\Lambda(t)$ is depicted in the panels. Note that results of the 4CC ansatz are shown in blue and results for the numerical solution of Schrödinger equation are shown in red.

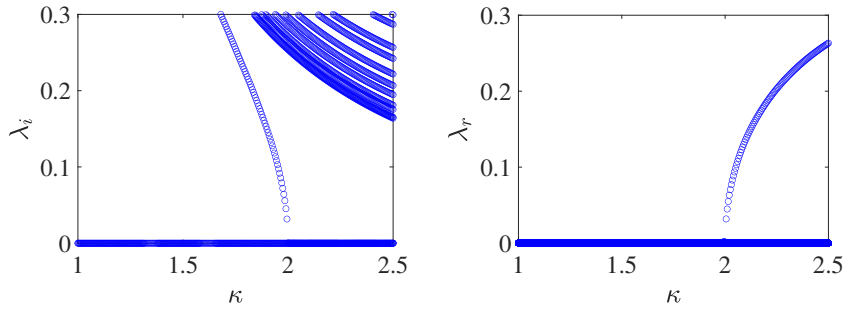


Figure 4. The imaginary λ_i (left) and real λ_r (right) parts of the eigenvalue λ as functions of κ with $g = 1$ and $\beta = 1$. At the critical value of $\kappa_c = 2$, the solution [cf. Eq. (4.1)] becomes unstable.

$$A_{12} = 2g\kappa \left[|\psi^{(0)}(x)|^2 + |\psi^{(0)}(-x)|^2 \right]^{\kappa-1} \left[(\psi^{(0)}(x))^2 + \psi_0(x)\psi_0(-x)\mathcal{P} \right], \quad (9.4a)$$

where \mathcal{P} stands for the space reflection operator, i.e., $\mathcal{P}f(x) = f(-x)$, for a general function $f(x)$.

The results of the eigenvalue problem [cf. Eq. (9.3)] are shown in Fig. 4 with $g = 1$

and $\beta = 1$. It can be discerned from the right panel of the figure, the emergence of a real eigenvalue at $\kappa_c = 2$, thus rendering the solution to be spectrally unstable (and similar to the local case). Although a detailed study and understanding of the underlying instability mechanism is of paramount importance (see, e.g., [32] as well as [33] and references therein), it is beyond the scope of the present work. Subsequently, Fig. 5 presents results on the spatio-temporal evolution of the exact solution for various values of κ . These numerical results were obtained by using a fourth-order accurate, central finite difference scheme for the (one-dimensional) Laplacian on a computational domain with half-width $L = 50$ and resolution $\Delta x = 0.1$. Note that Fig. 5(d) demonstrates an unstable solution (i.e., a blowup case), and the time integration was stopped when the full-width-at-half-maximum (FWHM) was less than Δx (for instance, the blow-up time happens at a later time $t_{\text{blowup}} \approx 474$ in this panel, as per the discretization employed herein.).

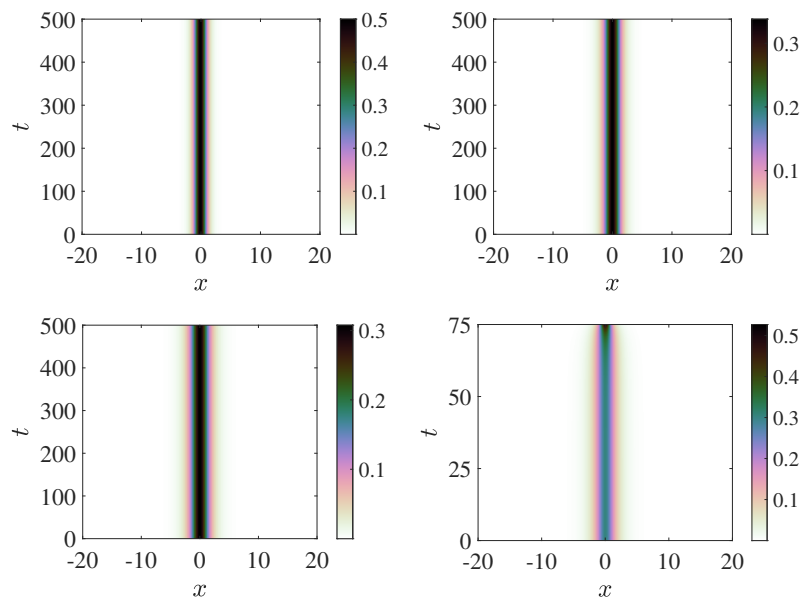


Figure 5. Spatio-temporal evolution of the density $|\psi|^2$ for values of κ of: $\kappa = 1$ (top left), $\kappa = 1.5$ (top right), $\kappa = 1.95$ (bottom left), and $\kappa = 2.1$ (bottom right).

10. Conclusions

In this work, we have considered the stability of the trapped soliton solution of a generalized Manakov system of two coupled nonlinear Schrödinger equations with the particular constraint $\psi_2(x, t) = \psi_1(-x, t)$ both numerically and analytically, and in a 2 and 4 collective coordinate (2CC and 4CC) approximation for arbitrary nonlinearity parameter κ . We were able to show that this system was equivalent to a nonlocal nonlinear Schrödinger equation derivable from a nonlocal action. We found by a variety of methods, that the stability to width changes of this NNLSE had exactly the same

behavior as the counterpart single component NLSE. That is, for $\kappa < 2$ there is stability, for $\kappa > 2$ there is instability (either collapse or blowup), and at $\kappa = 2$, there is a critical mass above which there is an instability. The exact solution is related to the critical mass. Unlike the NLSE which has Galilean invariance and a conserved momentum which can be nonzero, the NNLSE has zero value for the conserved momentum as well as having some potentially complex conserved normalization factors. This leads to a different response to shifting the initial conditions on the wave function to be slightly different than zero. When we add a nonzero ‘chirp’ term to the phase of the exact solution, we find that this adds extra energy to the soliton which then results in the soliton width having oscillations which are in accordance with this extra energy. For the NNLSE parity is conserved and the total momentum is zero. The system does not have Galilean invariance. When we shift the soliton slightly from the origin, the ensuing oscillations are reasonably well captured by the 4CC approximation which violates parity conservation. In conclusion, we have mapped out the stability regions for the NNLSE with arbitrary nonlinearity parameter κ and have studied the response of the exact solutions both analytically (in the realm of a collective coordinate approximation) as well as numerically, and found the two approaches are in accordance.

Acknowledgments

We thank M. Lakshmanan (Bharathidasan University) for useful correspondence. EGC, FC, and JFD would like to thank the Santa Fe Institute and the Center for Nonlinear Studies at Los Alamos National Laboratory for their hospitality. AK is grateful to Indian National Science Academy (INSA) for awarding him INSA Senior Scientist position at Savitribai Phule Pune University, Pune, India. The work of AS was supported by the U.S. Department of Energy.

Appendix A. Useful integrals and identities

$$c_1(\gamma) = \int_{-\infty}^{+\infty} dz \operatorname{sech}^{2\gamma}(z) = \frac{\sqrt{\pi} \Gamma[\gamma]}{\Gamma[\gamma + 1/2]}, \quad (\text{A.1a})$$

$$\begin{aligned} c_2(\gamma) &= \int_{-\infty}^{+\infty} dz z^2 \operatorname{sech}^{2\gamma}(z) \\ &= 2^{2\gamma-1} {}_4F_3[\gamma, \gamma, \gamma, 2\gamma; 1 + \gamma, 1 + \gamma, 1 + \gamma; -1]/\gamma^3, \end{aligned} \quad (\text{A.1b})$$

$$\begin{aligned} c_3(\gamma) &= \int_{-\infty}^{+\infty} dz \operatorname{sech}^{2\gamma}(z) \tanh^2(z) \\ &= c_1(\gamma) - c_1(\gamma + 1) = \frac{c_1(\gamma)}{2\gamma + 1}. \end{aligned} \quad (\text{A.1c})$$

A useful result is

$$\frac{c_1(\gamma + 1)}{c_1(\gamma)} = \frac{2\gamma}{2\gamma + 1}. \quad (\text{A.2})$$

We have defined the integral $f(z, \kappa)$ in (8.5):

$$f(z, \gamma) = \frac{2\gamma + 1}{2^{1/\gamma+2} \gamma c_1(\gamma)} \int dy [\operatorname{sech}^{2\gamma}(y - z) + \operatorname{sech}^{2\gamma}(y + z)]^{1/\gamma+1}. \quad (\text{A.3})$$

Then

$$f(0, \gamma) = \frac{2\gamma + 1}{2\gamma c_1(\gamma)} \int dy \operatorname{sech}^{2\gamma+2}(y) = \frac{2\gamma + 1}{2\gamma} \frac{c_1(\gamma + 1)}{c_1(\gamma)} = 1. \quad (\text{A.4})$$

Plots of $f(z, \gamma)$ are shown in the left panel in Fig. A1. The derivative of $f(z, \gamma)$ wrt z is given by

$$f'(z, \gamma) = \frac{(\gamma + 1)(2\gamma + 1)}{2^{1/\gamma+1} \gamma c_1(\gamma)} \int dy [\operatorname{sech}^{2\gamma}(y - z) + \operatorname{sech}^{2\gamma}(y + z)]^{1/\gamma} \times [\operatorname{sech}^{2\gamma}(y - z) \tanh(y - z) - \operatorname{sech}^{2\gamma}(y + z) \tanh(y + z)], \quad (\text{A.5})$$

where $f'(0, \gamma) = 0$. Plots of $f'(z, \gamma)$ are shown in the right panel in Fig. A1. A short calculation using Mathematica gives

$$f''(0, \gamma) = -4 \frac{\gamma + 1}{2\gamma + 3}. \quad (\text{A.6})$$

Expanding $f(z, \gamma)$ about the origin gives

$$f(z, \gamma) = f(0, \gamma) + f'(0, \gamma) z + \frac{1}{2} f''(0, \gamma) z^2 + \dots = 1 - 2 \frac{\gamma + 1}{2\gamma + 3} z^2 + \dots, \quad (\text{A.7a})$$

$$f'(z, \gamma) = -4 \frac{\gamma + 1}{2\gamma + 3} z + \dots. \quad (\text{A.7b})$$

Appendix B. Moments and collective coordinates

The variational wave function of Eq. (8.1a) is of the form

$$\psi(x, t) = \left[\frac{M}{G(t) c_1(\gamma)} \right]^{1/2} \operatorname{sech}^\gamma \left[\frac{x - q(t)}{G(t)} \right] e^{i\phi(x, t)}, \quad (\text{B.1a})$$

$$\phi(x, t) = p(t) (x - q(t)) + \Lambda(t) (x - q(t))^2. \quad (\text{B.1b})$$

Let us define the n^{th} moment of the density distribution by

$$\begin{aligned} M_n(t) &= \int_{-\infty}^{+\infty} dx x^n |\psi(x, t)|^2 \\ &= \frac{M}{G(t) c_1(\gamma)} \int_{-\infty}^{+\infty} dx x^n \operatorname{sech}^{2\gamma}[(x - q(t))/G(t)] \\ &= \frac{M}{c_1(\gamma)} \int_{-\infty}^{+\infty} dy [G(t) y + q(t)]^n \operatorname{sech}^{2\gamma}(y). \end{aligned} \quad (\text{B.2})$$

Explicitly, we find:

$$M_0(t) = M, \quad (\text{B.3a})$$

$$M_1(t) = M q(t), \quad (\text{B.3b})$$

$$M_2(t) = M \left[q^2(t) + G^2(t) \frac{c_2(\gamma)}{c_1(\gamma)} \right], \quad (\text{B.3c})$$

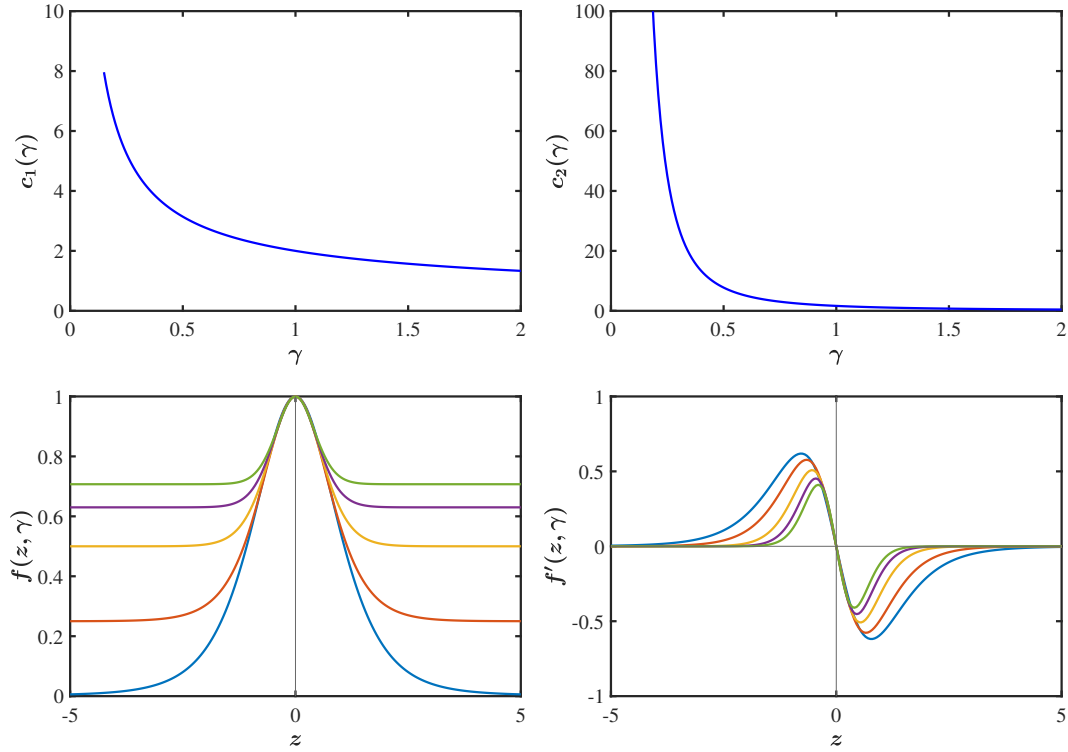


Figure A1. The top panels present $c_1(\gamma)$ (left panel) and $c_2(\gamma)$ (right panel) as a function of γ (for their definition, see Eqs. (A.1a) and (A.1b), respectively). The bottom panels demonstrate the dependence of $f(z, \gamma)$ (left panel), and $f'(z, \gamma)$ (right panel) on z , and for various values of $\gamma = 0.1, 0.5, 1, 1.5$, and 2 depicted by solid blue, orange, yellow, purple, and green lines, respectively (see Eqs. (A.3) and (A.5), respectively).

from which we can find $q(t)$ and $G(t)$. The zeroth moment, i.e., the mass of the soliton must be conserved. In a similar way, let us define the n^{th} moment of the momentum distribution by

$$\begin{aligned}
 P_n(t) &= \frac{1}{2i} \int_{-\infty}^{+\infty} dx x^n \left[\psi^*(x, t) \frac{\partial \psi(x, t)}{\partial x} - \frac{\partial \psi^*(x, t)}{\partial x} \psi(x, t) \right] \\
 &= \int_{-\infty}^{+\infty} dx x^n \operatorname{Im} \left\{ \psi^*(x, t) \frac{\partial \psi(x, t)}{\partial x} \right\} = \int_{-\infty}^{+\infty} dx x^n \frac{\partial \phi(x, t)}{\partial x} |\psi(x, t)|^2 \\
 &= \int_{-\infty}^{+\infty} dx x^n \{ p(t) + 2 \Lambda(t) [x - q(t)] \} |\psi(x, t)|^2 \\
 &= \frac{M}{G(t) c_1(\gamma)} \int_{-\infty}^{+\infty} dx x^n \{ p(t) + 2 \Lambda(t) [x - q(t)] \} \operatorname{sech}^{2\gamma} [(x - q(t))/G(t)] \\
 &= \frac{M}{c_1(\gamma)} \int_{-\infty}^{+\infty} dy [q(t) + G(t) y]^n [p(t) + 2 \Lambda(t) G(t) y] \operatorname{sech}^{2\gamma}(y) .
 \end{aligned} \tag{B.4}$$

Explicitly, we find:

$$P_0(t) = M p(t), \quad (\text{B.5a})$$

$$P_1(t) = M \left[p(t) q(t) + 2 \Lambda(t) G^2(t) \frac{c_2(\gamma)}{c_1(\gamma)} \right]. \quad (\text{B.5b})$$

This way, $p(t)$ can be obtained from (B.5a), and $\Lambda(t)$ from:

$$\Lambda(t) = \frac{1}{2 G^2(t)} \left[\frac{P_1(t)}{M} - p(t) q(t) \right] \frac{c_1(\gamma)}{c_2(\gamma)}. \quad (\text{B.6})$$

References

- [1] P.G. Kevrekidis and D.J. Frantzeskakis, Solitons in coupled nonlinear Schrödinger models: A survey of recent developments, *Rev. Phys.* **1** (2016), 140. <https://doi.org/10.1016/j.revip.2016.07.002>.
- [2] V.V. Konotop and D.A. Zezyulin, Spectral singularities of odd- \mathcal{PT} -symmetric potentials, *Phys. Rev. A* **99** (2019), 013823. doi:10.1103/PhysRevA.99.013823.
- [3] F. Cooper, A. Khare, A. Comech, B. Mihaila, J.F. Dawson and A. Saxena, Stability of exact solutions of the nonlinear Schrödinger equation in an external potential having supersymmetry and parity-time symmetry, *J. Phys. A: Math. Theor.* **50** (2017), 015301.
- [4] F. Cooper, J.F. Dawson, F.G. Mertens, E. Arévalo, N.R. Quintero, B. Mihaila, A. Khare and A. Saxena, Response of exact solutions of the nonlinear Schrödinger equation to small perturbations in a class of complex external potentials having supersymmetry and parity-time symmetry, *Journal of Physics A: Mathematical and Theoretical* **50**(48) (2017), 485205. <http://stacks.iop.org/1751-8121/50/i=48/a=485205>.
- [5] E.G. Charalampidis, J.F. Dawson, F. Cooper, A. Khare and A. Saxena, Stability and response of trapped solitary wave solutions of coupled nonlinear Schrödinger equations in an external \mathcal{PT} - and supersymmetric potential, *Journal of Physics A: Mathematical and Theoretical* **53**(45) (2020), 455702. doi:10.1088/1751-8121/abb278.
- [6] E.G. Charalampidis, F. Cooper, J.F. Dawson, A. Khare and A. Saxena, Behavior of solitary waves of coupled nonlinear Schrödinger equations subjected to complex external periodic potentials with odd-PT symmetry, *Journal of Physics A: Mathematical and Theoretical* **54**(14) (2021), 145701. doi:10.1088/1751-8121/abdca8.
- [7] S.V. Manakov, On the theory of two-dimensional stationary self-focusing of electromagnetic waves, *Zh. Eksp. Teor. Fiz.* **65** (1973), 505, [Sov. Phys. JETP **38**, 248 (1974)].
- [8] J. Ablowitz and Z.H. Musslimani, Integrable nonlocal nonlinear Schrödinger equation, *Phys. Rev. Lett.* **110** (2013), 064105.
- [9] M.J. Ablowitz and Z.H. Musslimani, Inverse scattering transform for the integrable nonlocal nonlinear Schrödinger equation, *Nonlinearity* **29**(3) (2016), 915–946. doi:10.1088/0951-7715/29/3/915.
- [10] V.S. Gerdjikov and A. Saxena, Complete integrability of nonlocal nonlinear Schrödinger equation, *Journal of Mathematical Physics* **58**(1) (2017), 013502.
- [11] S. Stalin, R. Ramakrishnan and M. Lakshmanan, Nondegenerate soliton solutions in certain coupled nonlinear Schrödinger systems, *Physics Letters A* **384**(9) (2020), 126201. doi:<https://doi.org/10.1016/j.physleta.2019.126201>.
- [12] M. Gurses and A. Pekcan, Nonlocal nonlinear Schrödinger equations and their soliton solutions, *Journal of Mathematical Physics* **59**(5) (2018), 051501.
- [13] W. Liu and X. Li, General soliton solutions to a (2+1)-dimensional nonlocal nonlinear Schrödinger equation with zero and nonzero boundary conditions, *Nonlinear Dynamics* **93**(2) (2018), 721–731.

- [14] B. Yang and Y. Chen, Dynamics of high-order solitons in the nonlocal nonlinear Schrödinger equation, *Nonlinear Dynamics* **94**(1) (2018), 489–502.
- [15] J. Yang, Physically significant nonlocal nonlinear Schrödinger equation and its soliton solutions, *Phys. Rev. E* **98** (2018), 042202. doi:10.1103/PhysRevE.98.042202.
- [16] K. Manikandan, S. Stalin and M. Senthilvelan, Dynamical behaviour of solitons in a invariant nonlocal nonlinear Schrödinger equation with distributed coefficients, *European Physical Journal B* **91**(11) (2018), 291.
- [17] B.-F. Feng, X.-D. Luo, M.J. Ablowitz and Z.H. Musslimani, General soliton solution to a nonlocal nonlinear Schrödinger equation with zero and nonzero boundary conditions, *Nonlinearity* **31**(12) (2018), 5385–5409.
- [18] N.V. Priya, M. Senthilvelan, G. Rangarajan and M. Lakshmanan, On symmetry preserving and symmetry broken bright, dark and antidark soliton solutions of nonlocal nonlinear Schrödinger equation, *Phys. Lett. A* **383**(1) (2019), 15–26.
- [19] J. Yang, General N-solitons and their dynamics in several nonlocal nonlinear Schrödinger equations, *Phys. Lett. A* **383**(4) (2019), 328–337.
- [20] S. Stalin, M. Senthilvelan and M. Lakshmanan, Energy-sharing collisions and the dynamics of degenerate solitons in the nonlocal Manakov system, *Nonlinear Dynamics* **95**(3) (2019), 1767–1780.
- [21] Y. Rybalko and D. Shepelsky, Long-time asymptotics for the integrable nonlocal nonlinear Schrödinger equation, *J. Math. Phys.* **60**(3) (2019), 031504.
- [22] T. Xu, S. Lan, M. Li, L.-L. Li and G.-W. Zhang, Mixed soliton solutions of the defocusing nonlocal nonlinear Schrödinger equation, *Physica D: Nonlinear Phenomena* **390** (2019), 47–61.
- [23] T. Xu, Y. Chen, M. Li and D.-X. Meng, General stationary solutions of the nonlocal nonlinear Schrödinger equation and their relevance to the PT-symmetric system, *Chaos* **29**(12) (2019), 123124.
- [24] D. Wang, Y. Huang, X. Yong and J. Zhang, Rational soliton solutions of the nonlocal nonlinear Schrödinger equation by the KP reduction method, *Int. J. Mod. Phys. B* **33**(30) (2019), 1950362.
- [25] J. Yang, *Nonlinear Waves in Integrable and Nonintegrable Systems*, Mathematical Modeling and Computation, Society for Industrial and Applied Mathematics (SIAM), Philadelphia, 2010.
- [26] G.H. Derrick, Comments on Nonlinear Wave Equations as Models for Elementary Particles, *Journal of Mathematical Physics* **5**(9) (1964), 1252–1254. doi:10.1063/1.1704233.
- [27] F. Cooper, H. Shepard, C. Lucheroni and P. Sodano, Post-Gaussian variational method for the nonlinear Schrödinger equation: Soliton behavior and blowup, *Physica D: Nonlinear Phenomena* **68**(3) (1993), 344–350. doi:https://doi.org/10.1016/0167-2789(93)90129-O. <http://www.sciencedirect.com/science/article/pii/0167278993901290>.
- [28] N.G. Vakhitov and A.A. Kolokolov, Stationary solutions of the wave equation in the medium with nonlinearity saturation, *Radiophys. Quantum Electron* **16** (1973), 783–789.
- [29] <https://www.mathworks.com/help/matlab/ref/ode113.html>.
- [30] A.-K. Kassam and L.N. Trefethen, Fourth-order time-stepping for stiff PDEs, *SIAM J. Sci. Comput.* **26**(4) (2005), 1214–1233. doi:10.1137/S1064827502410633.
- [31] C.T. Kelley, *Solving Nonlinear Equations with Newton's Method*, Fundamentals of Algorithms, Society for Industrial and Applied Mathematics (SIAM), Philadelphia, 2003.
- [32] C. Sulem and P.L. Sulem, *The Nonlinear Schrödinger Equation: Self-Focusing and Wave Collapse*, Applied Sciences, Springer-Verlag, New York, 1999.
- [33] C.I. Siettos, I.G. Kevrekidis and P.G. Kevrekidis, Focusing revisited: a renormalization/bifurcation approach, *Nonlinearity* **16**(2) (2003), 497–506. doi:10.1088/0951-7715/16/2/308.